Ionization Thresholds and Residue Removal in Inductively Coupled Etching of NiO/Ga_2O_3 with Ar and BCl_3

Chao-Ching Chiang[1], Xinyi Xia[1], Jian-Sian Li[1], Fan Ren[1], and S.J. Pearton[2]

[1]Department of Chemical Engineering, University of Florida, Gainesville, FL 32606 USA
[2]Department of Materials Science and Engineering, University of Florida, Gainesville, FL 32606 USA
Email: cchiang@ufl.edu, Phone: 352-328-5477

Keywords: Ga_2O_3, NiO, BCl_3, ICP etch, dry etch, etch residue

Abstract

BCl_3 is an attractive plasma etchant for oxides because it is a Lewis acid used to scavenge native oxides on many semiconductors due to the strong B-O bonding. We investigated BCl_3-based dry etching of the NiO/Ga_2O_3 heterojunction system. BCl_3/Ar Inductively Coupled Plasmas produced maximum etch rates for NiO up to 300 Å.min^{-1} and 800 Å.min^{-1} for β-Ga_2O_3 under moderate plasma power conditions suitable for low damage pattern transfer. The selectivity for NiO: Ga_2O_3 was less than one under all conditions. The ion energy threshold for initiation of the etching of NiO was between 35-60 eV, depending on the condition and the etch mechanism was ion-driven, as determined by the linear dependence of etch rate on the square root of ion energy incident on the surface. By sharp contrast, the etching of Ga_2O_3 had a stronger chemical component, without a well-defined ion energy threshold. The as-etched NiO and Ga_2O_3 surfaces show chlorine residues, which can be removed on both materials by the standard 1 NH_4OH: 10 H_2O or 1 HCl: 10 H_2O rinses used for native oxide removal. According to the location of the Cl $2p_{3/2}$ peak on the XPS analysis, the Cl is ionically bonded.

Introduction

One of the major drawbacks of β-Ga_2O_3 is the lack of p-type dopants with shallow ionization energies.[1-4] This means that at room temperature, the maximum hole concentration is impractically low, although, native p-type conductivity can be observed at high temperatures due to native Ga vacancies (V_{Ga}), which are acceptors.[3,5-7] An alternative approach is to use p-type oxides, such as Cu_2O[8] or NiO[9-11], to form heterojunctions with n-type Ga_2O_3. In particular, NiO provides a relatively wide process window, where the electrical properties can be tuned by the deposition parameters.[12,13] Both power rectifiers[10,11,14-23] and UV photodetectors[9] have been demonstrated in this system. Common to any device structure is the need to pattern the NiO and possibly the Ga_2O_3. There are some initial studies of dry etching of Ga_2O_3 but little on heterojunctions with NiO or on the etch residues remaining on the surface.[24-28] Etch rates of NiO were reported to be only 100 nm.min^{-1} in Inductively Coupled Plasmas (ICP) using Cl_2/Ar or BCl_3/Ar chemistries.[29] Instead of the Cl_2 plasma chemistry typically used for Ga_2O_3,[30-32] substitution with BCl_3 gas should have advantages because the B–O bonding of 8.39 eV is much stronger than the Cl–O bonding of 2.82 eV. The latter is too weak to form a reactive layer with oxygen in metal oxides.[33] This means that BCl_3 is widely employed to remove native oxides on semiconductors and prevent incubation delays where the prevalent chlorine plasma cannot break through the native oxide.[34]

In this paper, we report the threshold ion energies for dry etching of NiO in BCl_3 discharges, the selectivity to β-Ga_2O_3, and the cleaning of chlorine-based residues remaining on the surface after plasma exposure. There was a threshold ion energy of ~35-60 eV for NiO dry etching, whereas Ga_2O_3 did not have discernable ion energy for initiation of etching, suggesting a stronger chemical etching component. Finally, standard surface cleaning steps were found to be effective in removing chlorine residues from the etched surfaces of both NiO and Ga_2O_3.

Experimental

The 190 nm thick NiO layers were deposited by magnetron sputtering on glass slides in a Kurt Lesker system at 3 mTorr working pressure and 150 W of 13.56 MHz power using two targets to achieve a deposition rate of around 2 Å.sec^{-1}. The O_2/Ar gas ratio was 1/10, producing polycrystalline films with a bandgap of 3.75 eV, resistivity of 0.1 Ω.cm, and density of 5.6 g.cm^{-3}. The β-Ga_2O_3 samples used were (100) bulk, Sn-doped substrates, grown by the Edge-Fed Defined Growth method and purchased from Novel Crystal Technology (Saitama, Japan). All the samples were patterned with PR1045 photoresist and etched in a PlasmaTherm 790 reactor. Discharges with 15 sccm of BCl_3 and 5 sccm of Argon at a fixed pressure of 5 mTorr were used to etch the NiO and Ga_2O_3. Etch rates were obtained by measuring the etch depth with a Tencor profilometer after the removal of the photoresist.

The near-surface composition of the NiO and Ga_2O_3 after dry etching was examined with X-Ray Photoelectron Spectroscopy (XPS), using a Physical Instruments ULVAC

PHI, with an Al x-ray source (energy 1486.6 eV, source power 300 W), analysis size of 100 μm diameter, a take-off angle of 50° and acceptance angle of ±7 degrees. The electron pass energy was 23.5 eV for high-resolution scans. The atomic percentages were calculated using CasaXPS software. To remove the chlorinated residues from the surface, we examined two standard cleaning mixtures, namely, $1NH_4OH$: $10H_2O$ or 1HCl: $10H_2O$ for 60 secs. Both of these rinses are used for native oxide removal.

Results and Discussion

Figure 1 shows the NiO and Ga_2O_3 etch rates in the BCl_3/Ar ICP discharges as a function of ICP source power at fixed rf chuck power of 150W. The chuck power controls the energies of the positive ions incident on the powered electrode where the samples sit, while the ICP power controls the ion density in the discharge. These ions will include Ar^+, as well as positively charged fragments of the BCl_3 molecules. As ICP power is increased the ion energy is decreased due to the increase in ion density. This is also shown in Figure 1. The dc bias decreases from about 380 V at 200W ICP power to ~270V at 600W ICP power. The ion energy is the sum of this self-bias, plus the plasma sheath potential, which is about 25V in this system. Thus, the average ion energies decrease from about 405eV to ~295 eV as ICP power increases from 200 to 600 W. The etch rates of both materials increase monotonically with ICP power, showing that the increased ion density more than compensates for the decrease in ion energy. The increase of the NiO and Ga_2O_3 etch rates with ICP source power is due to the increase of the positive ion density. The etch rate of NiO is smaller than that of Ga_2O_3 for all ICP powers investigated, which is consistent with a lower degree of chemical etch component.

The selectivity for etching one material over another is simply the ratio of their etch rates under the same conditions. Figure 3 (a) shows the NiO/Ga_2O_3 selectivity as a function of rf power at the lowest ICP power we used, 150 W. The selectivity is essentially constant over the range of rf powers investigated. However, at higher rf powers, the selectivity increases, as shown in Figure 3 (b). This shows that the ion energy is the dominant factor determining the selectivity above a certain threshold ion energy, while the selectivities are almost independent of plasma density. The selectivity for etching NiO is always <1, which is not desirable for selective patterning of NiO films on Ga_2O_3. The two approaches for overcoming this would be to use low etch rate conditions and carefully restrict the over-etch time during the plasma exposure time, or to include a thin etch stop layer between the NiO and the Ga_2O_3 which could then be selectively removed by a wet etch step.

For etch processes where the ion-assisted etching mechanism is important, the etch rate (ER) is given by[35-37]

$$ER = (J_+ A_{sat}(\sqrt{E} - \sqrt{E_{th}}\ )$$

where J_+ is the positive ion flux, A_{sat} is a proportionality constant dependent on the specific plasma-material combination, E is the ion energy, and E_{th} is the threshold energy for initiation of etching. Figure 3 (a) shows there is a linear relationship between the etch rate of both NiO and Ga_2O_3 versus the square root of ion energy. This suggests the etching for both materials are ion-flux limited.[35-37] The intercept in plots like Figure 3 (a) is the approximate threshold ion energy.[33] This analysis worked for the NiO, with E_{th} being ~35-60 eV for BCl_3/Ar in our system. These are fairly similar to the reported threshold ion energies for etching NiO in Cl2/Ar.[28]

However, this approach did not work for Ga_2O_3 samples in Figure 3 (a), where the plot has a negative intercept on the x-axis, which indicates there is also a significant chemical etching component. Similarly, under conditions of low rf power, corresponding to low ion energy, neither material showed a realistic threshold within the analysis above, since the slopes are negative in Figure 3 (b). These are conditions where chemical etching plays a more significant role.

An expanded view of the Cl 2p peaks of the Survey XPS spectra from the two types of materials after etching and after subsequent cleaning in either $1NH_4OH$: $10H_2O$ or 1HCl: $10H_2O$ rinse is shown in Figure 4 (a) for NiO and Figure 4 (b) for Ga_2O_3. The Cl bonds are likely to be metal bonds rather than covalent bonds according to the location of the Cl 2p peak.[38,39] Table I summarizes the near-surface atomic compositions of the samples before and after the cleaning rinses. The NiO has 15.7 % Cl in this near-surface region, much higher than the 3.7% on the Ga_2O_3 surface. This is consistent with the lower etch rates and lower volatilities of the $NiCl_x$ etch products. Note that both cleaning procedures are effective in completely removing the chlorine-related surface residues. These are both standard processes for removing native oxides on compound semiconductor surfaces, so they fit well into any device processing sequence that includes a dry etching step.[40,41]

TABLE I
NEAR-SURFACE COMPOSITIONS OF NIO AND GA_2O_3 SAMPLES AFTER EXPOSURE TO BCL_3/AR PLASMAS AND THEN SUBSEQUENT CLEANING IN NH_4OH OR HCL RINSE.

Samples	Atomic percentage (%)			
	O 1s	C 1s	Ni 2p	Cl 2p
NiO as-etched	55.42	11.07	17.81	15.70
HCl cleaned	62.05	8.65	29.3	0
NH_4OH cleaned	69.87	8.4	21.51	0.22
Samples	Atomic percentage (%)			
	O 1s	C 1s	Ga 2p3	Cl 2p
Ga_2O_3 as-etched	68.88	10.27	17.21	3.73
HCl cleaned	35.07	0	64.93	0
NH_4OH cleaned	39.27	0	60.73	0

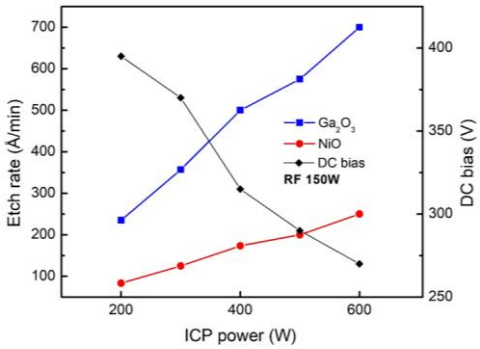

Figure 1. Etch rate of NiO and Ga_2O_3 in BCl_3/Ar discharges as a function of ICP power at fixed rf power of 150 W. The dc self-bias developed on the electrode is also shown.

(a)

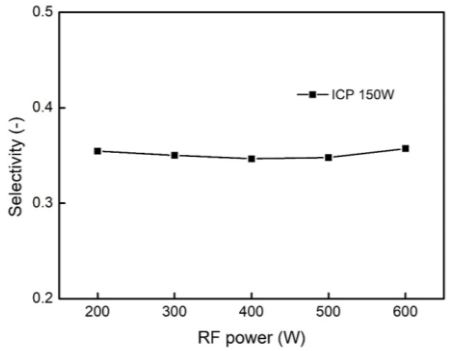

(b)

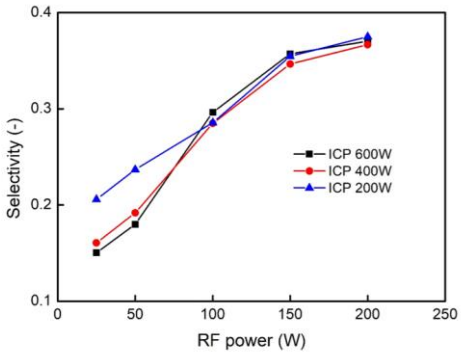

Figure 2. Etch rate of (a) NiO and (b) Ga_2O_3 in BCl_3/Ar discharges as a function of rf power at various ICP powers in the range of 200-600 W. The dc self-bias developed on the electrode is also shown in (c).

(a)

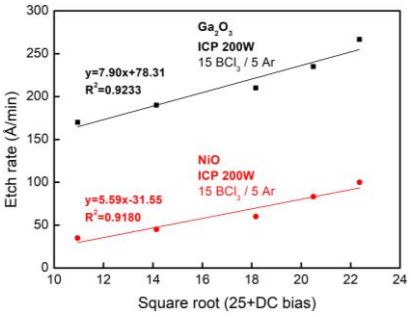

(b)

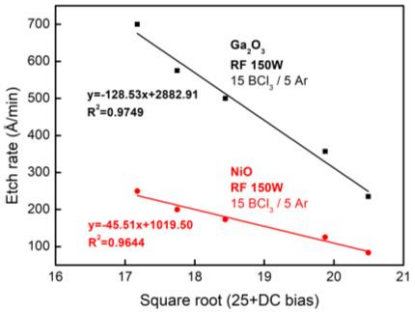

Figure 3. Etch rates for NiO and Ga_2O_3 as a function of $(25 + \text{dc bias})^{0.5}$, which approximates ion energy for (a) different rf powers or (b) different ICP powers.

(a)

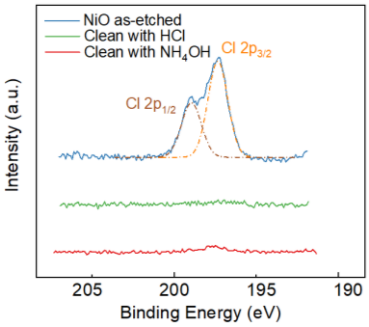

(b)

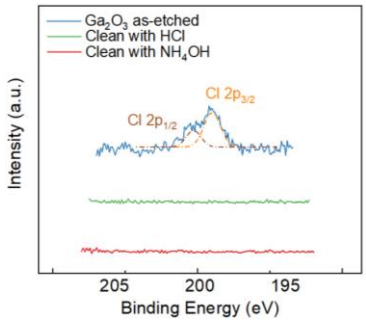

Figure 4. Expanded view of Cl 2p transitions in XPS spectra from (a) NiO and (b) Ga_2O_3 after exposure to the BCl_3/Ar discharge and then subsequent cleaning in either HCl or NH_4OH.

CONCLUSIONS

The use of NiO with n-type Ga_2O_3 has shown promising device results, but the details, such as the choice of plasma chemistry for dry etching, the threshold ion energies for etching, and the subsequent surface cleaning processes have been lacking. The use of the BCl_3/Ar plasma chemistry is attractive because of the scavenging effect of this Lewis acid on native oxides. We found this chemistry has selectivity <1 for NiO over Ga_2O_3, with an ion-flux-limited regime operative for NiO over a wide range of conditions. For NiO, the etch rate is independent of the reactive neural flux in the ion-flux-limited regime. Standard surface cleaning rinses were found to be effective in removing chlorinated residues. There is more scope for modification of surface properties using plasma processes, as there have been recent reports the valence and conduction band offsets of the NiO_x/β-Ga_2O_3 heterojunction decrease with F plasma pre-treatment.[40-42]

ACKNOWLEDGMENTS

The work at UF was performed as part of the Interaction of Ionizing Radiation with Matter University Research Alliance (IIRM-URA), sponsored by the US Department of Defense, Defense Threat Reduction Agency under the award HDTRA1-20-2-0002. The content of the information does not necessarily reflect the position or the policy of the federal government, and no official endorsement should be inferred. The work at UF was also supported by NSF DMR 1856662 (James Edgar).

REFERENCES

[1] A. Mock et al., *Phys Rev B*, **96**, 14 (2017).
[2] S.I. Stepanov et al., *Rev Adv. Mater. Sci.*, **44**, 63 (2016).
[3] B.E. Kananen et al., *J. Appl. Phys.*, **122**, 6 (2017).
[4] E. Chikoidze et al., *J. Mater. Chem.*, **C7**, 10231 (2019).
[5] A. Goyal et al., *J. Appl. Phys.*, **129**, 245704 (2021).
[6] E. Chikoidze et al., *Materials Today Phys.*, **3**, 118 (2017).
[7] S. Modak et al., *Appl. Phys. Lett.*, **120**, 233503 (2022).
[8] S. Modak et al., *APL Mater.*, **10**, 031106 (2022).
[9] T. Watahiki et al., *Appl. Phys. Lett.*, **111**, 222104 (2017).
[10] J. Zhang et al., *ACS Appl. Electron. Mater.*, **2**, 456 (2020).
[11] Y. Lv et al., *IEEE Trans Power Electron.*, **36**, 6179 (2021).
[12] H. Gong et al., *Appl. Phys. Lett.*, **117**, 022104 (2020).
[13] M. Napari et al., *InfoMat.*, **3**, 536 (2021).
[14] J. A. Spencer et al., *Appl. Phys. Rev.*, **9**, 011315 (2022).
[15] X. Lu et al., *IEEE Electron Dev. Lett.*, **41**, 449 (2020).
[16] C. Wang et al., *IEEE Electron Dev. Lett.*, **42**, 485 (2021).
[17] Q. Yan et al., *Appl. Phys. Lett.*, **118**, 122102 (2021).
[18] H. Gong et al., *IEEE Trans. Power Electron.*, **36**, 12213 (2021).
[19] H. Gong et al., *Appl. Phys. Lett.*, **118**, 202102 (2021)
[20] W. Hao et al., *Appl. Phys. Lett.*, **118**, 043501 (2021).
[21] F. Zhou et al., *IEEE Trans. Power Electron.*, **37**, 1223 (2022).
[22] Q. Yan et al., *Appl. Phys. Lett.*, **120**, 092106 (2022).
[23] Y. Wang et al., *IEEE Trans. Power Electron.*, **37**, 3743 (2022).
[24] J-S. Li et al., *Appl. Phys. Lett.*, **121**, 042105 (2022).
[25] J. Yang et al., *J. Vac. Sci. Technol. B*, **36**, 061201 (2018).
[26] J. E. Hogan et al., *Semicond. Sci. Technol.*, **31**, 065006 (2016).
[27] Y. Zhang et al., *Appl. Phys. Lett.*, **115**, 013501 (2019).
[28] C-C. Chiang et al., *ECS J. Solid State Sci. Technol.*, **11**, 104001 (2022)
[29] H. N. Cho et al., *Electrochem. Solid-State Lett.*, **11**, D23 (2008).
[30] A.P. Shah and A. Bhattacharya, *J. Vac. Sci. Technol.*, **35**, 041301 (2017).
[31] H-C. Huang et al., *J. Mater. Res.*, **36**, 4756 (2021).
[32] H. Okumura and T. Tanaka, *Japan J. Appl. Phys.*, **58**, 120902 (2019).
[33] J. B. Park et al., *J. Korean Phys. Soc.*, **54**, 976 (2009).
[34] *Handbook of Advanced Plasma Processing Techniques*, R.J. Shul and S.J. Pearton (Springer, Berlin, 2000).
[35] L. Stafford et al., *Appl. Phys. Lett.*, **87**, 071502 (2000).
[36] C. Steinbruchel, *Appl. Phys. Lett.*, **55**, 1960 (1989).
[37] S. J. Pearton et al., *J. Vac. Sci. Technol. A*, **38**, 020802 (2020).
[38] C. D. Wagner et al., NIST Standard Reference Database 20, Version 3.4 (http:/srdata.nist.gov/xps/), (2003).
[39] I. Bello et al., *J. Appl. Phys.*, **75**, 3092 (1994).
[40] X. Xia et al., *J. Phys. D*, **55**, 385105 (2022).
[41] Y. Xiao et al., *Appl. Surf. Sci.*, **578**, 152047 (2022).
[42] J. B. Varley et al., *Physical Review B*, **85**, 081109 (2012).